Conductive fillers for electroactive shape memory actuators

Anchista Sakulmankongsuk, S3563723
Supervisors: Dr. Ranjita Bose and Felipe Orozco Gutierrez
University of Groningen
June 2021

Abstract
Conductivity, thermo-mechanical properties, shape memory ability, along with economics of multi-walled carbon nanotube (CNT)/carbon black (CB) filled composite were investigated. 8 wt% CNT/CB of different ratios were formulated on furan-grafted polyketone (PK30-Fu) reversibly cross-linked with bis-maleimide (Bis-Ma) through Diels-Alder chemistry. The cross-linked composites were identified with H-NMR and FT-IR. Linear positive correlation was observed between surface temperature detected, current and conductivity. Samples with more CB content exhibit greater current and conductivity, and higher temperature profile as a result of successful resistive heating. No synergies were found regarding the conductivity between CNT and CB as co-fillers for the prepared system. The most conductive sample (CNT0/CB100) showed highest recovery rate, partial reprogrammability and good shape recovery for the new permanent shape. Shape recovery rate also forms linear positive interrelationship with temperature and current. All formulations acquired similar complex modulus (G*) and 100% shape recovery ratio. Both performance (electrical properties, shape memory ability) and economics are consistent, as the formulation with the best performance is also the cheapest.

1. Introduction

Shape memory polymer refers to polymers whose shape and structure can be programmed to a temporary shape, and changes back to the original shape when triggered by certain stimuli such as light, heat, pH, moisture or magnetism [1]. They possess some advantages over other shape memory materials including low cost, low density, high elastic deformation, possibly biodegradation and biocompatibility. Application of these materials includes biomedical devices such as medical casts and implants, self-tightening sutures and drug delivery capsules [2,3], deployable structures like soft robotics actuators [4] or heat shrinkable packages [5]. For shape memory polymers, heat is the most common trigger for the shape programming and recovery.

Specific processing conditions are required to achieve the shape memory effect.
In short, strained temporary shape must be separated, and original shape recovery must be triggered through “reversible net points” [1]. Typical approach to preserve the temporary shape is depicted in **Figure 1a**. First, the material is cooled below its glass transition (T_g) or melting temperature (T_m) where the structure is “frozen” in its stressed state (1-3 in **Figure 1a**). Subsequently, the original shape is recovered upon heating above the transition temperature previously used to “freeze” the temporary shape (4-5 in **Figure 1a**). Shape reprogramming is also possible through reversible binding groups (RBGs) in the polymer structure; these groups serve to stabilize the temporary shape while also introducing new and recyclable permanent shapes as shown in **Figure 1b**. RBGs can be either non-covalent such as hydrogen bonding, ionic interaction, $\pi - \pi$ stacking, or covalent such as transesterification, addition fragmentation and Diels-Alder (DA) [4+2] cycloaddition (mechanism displayed in **Figure 2**). The Diels-Alder pathway is especially advantageous as it allows the formation of a reversible

three-dimensional network through its forward (DA) and reverse (retro-DA) reaction [6]. Also particularly, the system can be chosen in such a way that the forward and reverse reaction fall into different temperature ranges, providing a high degree of control towards the cross-linking process.

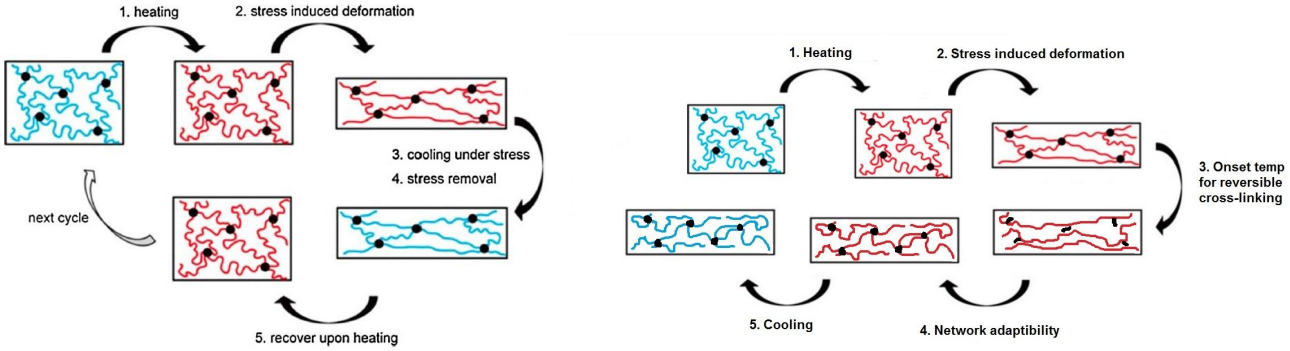

Figure 1. Conventional shape memory mechanism [7] (a) and shape reprogramming employing RBGs (b). The blue polymer represents the polymer below its T_g and the red polymer above its T_g. The black dots are the cross-linkages in the polymer matrix.

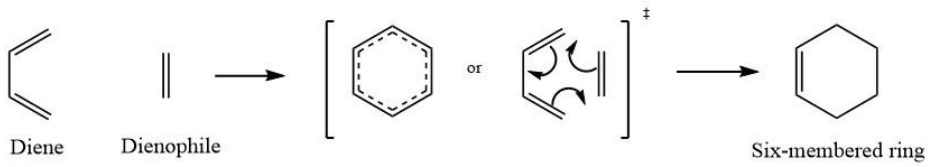

Figure 2. Diels-Alder [4+2] cycloaddition mechanism [8].

Polymers containing RBGs not only exhibit shape memory features, but also potentially self-healing abilities [5]. Materials with self-healing characteristics can repair damages from micro cracks or scratches within itself automatically without any manual interference [9,10]. Polymers with this ability are called self-healing polymers, and are considered a potential solution for many polymer degradation problems, especially in adhesives. Once cracks are initiated, they often propagate within the polymeric structure resulting in its mechanical properties being compromised, possibly to the point of failures. Often with these types of damages deep within the polymer matrix, detection and repair is almost impossible [10]. Self-healing polymers are therefore important and valuable, since the ability to repair the small damages before they propagate further will minimize maintenance and ensure longer lifetime. Self-healing mechanism employing RBGs is depicted in **Figure 3**.

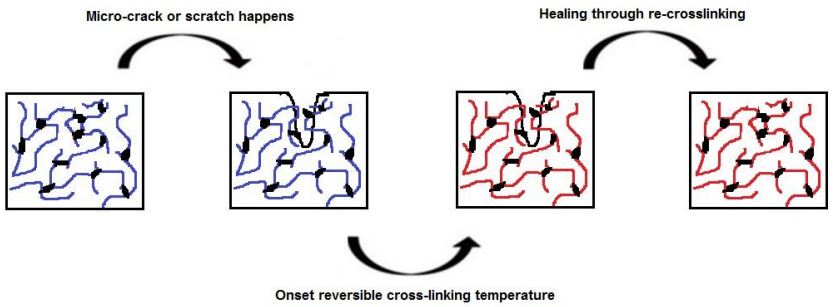

Figure 3. Self-healing mechanism of the reversible cross-linked thermoset polymer.

Based on previous works, shape memory and self-healing abilities were achievable with thermo-reversible Diels-Alder based thermoset [1,6,11-13]. With Diels-Alder chemistry, the cross-linking (binding) process is reversible, it is therefore capable of activating the shape memory effect and also reprogrammability (mechanisms in **Figure 1**). Due to the associated state of the linkages lies in the lower temperature range (50-70°C) [14] than the dissociated state (110-170°C) [14,15]. The cross-linked network is then able to adapt itself while being deformed by dissociating (via retro-DA) at elevated temperature and reassociating (via DA) upon cooling down. As a result, a new stable network and reprogrammed permanent shape of the thermoset is formed, majorly contributing to the recyclability of the shape memory polymer. Moreover, its reversible nature also promotes self-healing mechanisms (**Figure 3**) as the binding groups can conveniently reassociate after broken at the cross-linking temperature for several times [13]. This is achievable because cracks most likely happen at the linkages rather than the polymer backbone.

The introduction of conductive fillers into the thermoset matrix enables its shape memory and self-healing effect to be induced via electrical current, rather than thermal heating [16]. The conductive fillers create a total pathway for electrical current to complete the circuit, and since polymers are poor conductors, the current passing through the material is generated as heat. Through “resistive heating”, the amount of heat can be controlled by regulating the voltage supply. Conductive polymers can be filled with carbon nanotubes (CNT) [6,12,16-24], carbon particles, hybrid conductive fiber, nickel chains and others [16]. The thermo-reversible Diels-Alder based thermoset has been researched in the context of conductive CNT-filled polymers [6,12]. However, due to its exceptional strength and conductivity, CNT is extremely high-priced. The focus of this study is then to explore an alternative towards conductive fillers used instead. Thus, multi-walled carbon nanotubes (CNT) and conductive carbon black (CB) will be investigated.

Multiwall-carbon nanotubes (CNT) cost approximately 2900 €/kg [25] whereas conductive carbon black (CB) costs about 120 €/kg [26]. Clearly, CB is much cheaper and more economical than CNT. CB is obtained through incomplete heavy petroleum processing while CNT is a synthetic material synthesized via chemical vapour deposition [27]. Carbon black is favourable economically, but the performance regarding conductivity and shape memory ability needs more investigation considering the results from different literature conducted on different polymers basis [19-21]. There has been a report on the synergistic effect of those two fillers combined, in which it is possible to achieve electrical resistivity values that were unattainable with a single nanofiller [18,24]. Also there, the addition of CB to CNT-filled composite effectively reduced the gaps between the CNT, resulting in a well-linked, solid conductive network [22]. Enhanced conductivity with hybrid composite was observed [20-21], however, there is no report yet of the conductivity, shape memory and self-healing abilities of furan-grafted polyketone filled with CNT/CB hybrid composite. Hence, the composite performances and also economic feasibility will be evaluated in this study.

Diels-Alder-based thermo-reversibly crosslinked polymer composites with different ratios of CNT and CB incorporated will be prepared and examined. The polymer system will be the furan-grafted polyketone (PK30-Fu) with 1,1-(methylenedi-4,1-phenylene)bis-maleimide (Bis-Ma) (schemes in **Figure 4** and **Figure**

5) [6,11-13]. Mechanical and electrical properties, shape memory abilities, reprogrammability, along with economic prospects of the final nanocomposite will be explored and compared in this study. Unfortunately, due to time constraints and other inconveniences, the self-healing test for this material will not be performed for this project.

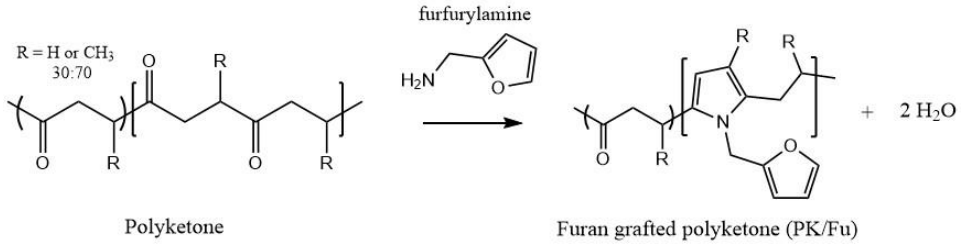

Figure 4. Paal-Knorr reaction of the polyketone (PK30) and furfurylamine.

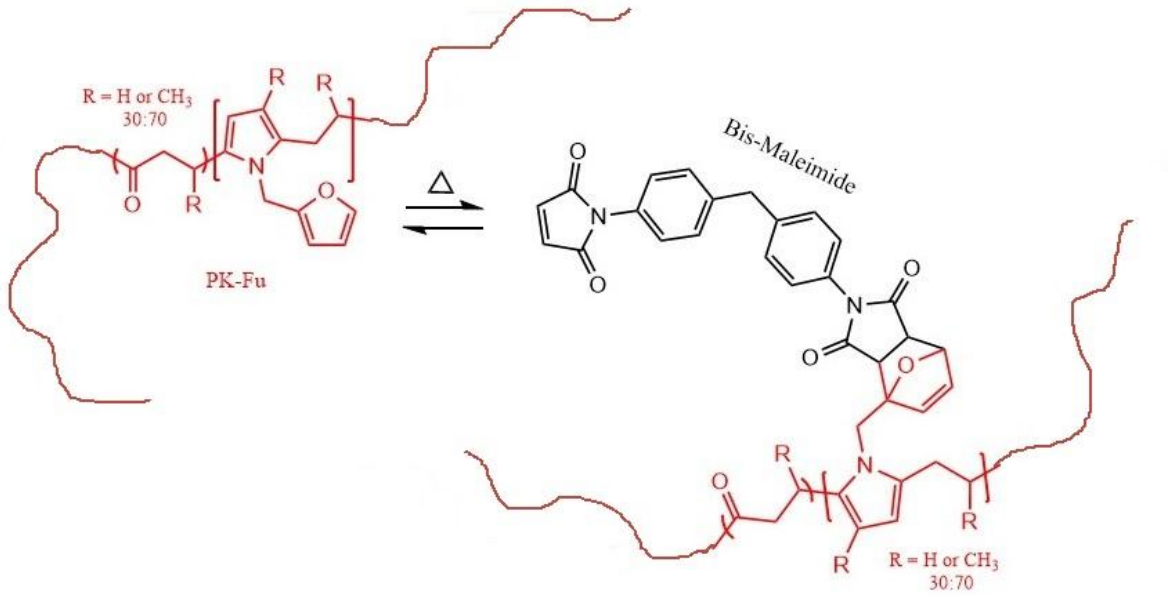

Figure 5. Diels-Alder's cycloaddition of the furan group on the grafted polyketone (PK-Fu) and the double bond on the end group of Bis-Ma.

2. Experimental - paragraph format includes all experimental details

2.1 Materials

Polyketone (PK30, Mw 2687 Da, 70% propylene:30% ethylene in the alkyl groups), furfurylamine (Fu, Sigma Aldrich, 99%, freshly distilled before used), 1,1-(methylenedi-4,1-phenylene)bis-maleimide (Bis-Ma, Sigma Aldrich, 95%), multi-walled carbon nanotubes (CNT, O.D. 6–9 nm with average length of 5 μm, Sigma Aldrich, 95% carbon), conductive carbon black (CB, Ketjenblack EC-600JD, Nouryon, 3 mm pellets, 30-50 nm carbon particles) and chloroform ($CHCl_3$, Sigma Aldrich, 99.5%) were used as obtained.

2.2 Functionalization of polyketone with furfurylamine via Paal-Knorr reaction

The polyketone (PK30, 48.51 g, 1 eq) and furfurylamine (7.16 g, 0.2 eq) was reacted at maximum of 20% 1,4-dicarbonyl conversion (C_{CO} = 0.2, see appendix A1.1) in a sealed round-bottom glass reactor with U-shape impeller and reflux condenser in an oil bath. Furfurylamine was added dropwise to the pre-heated liquid polyketone at the reaction temperature (110 °C) with 590 rpm stirring speed. The colour changed from copper brown to deep red to orange throughout the 3 hour reaction time. Approximately 150 mL of chloroform was added to dissolve the crude furan functionalized polyketone (PK30-Fu) at room temperature overnight. The chloroform was later evaporated over the rotary evaporator. The dried furan-grafted polyketone product is a viscous reddish brown polymer.

2.3 DA reaction with Bis-Ma and conductive composite formulation of the furan functionalized polyketone

The conductive fillers in this project are carbon nanotubes (CNT) and carbon black (CB) (5 formulations: CNT100, CNT75/CB25, CNT50/CB50, CNT25/CB75 and CB100). First, the conductive filler (8 wt% of the composite product) was dispersed in chloroform (0.5 vol%) via sonication for 0.5 hour. In the meantime, the furan-grafted polyketone (PK30-Fu, 7 g) was dissolved in chloroform (10 vol%) in a round bottom flask. Once dispersed, the conductive fillers (CNT or CB) dispersion was immediately transferred to the PK30-Fu solution at 50 °C and stirred at 500 rpm for 2 hours with a magnetic stirrer equipped with a reflux condenser in an oil bath. Subsequently, Bis-Ma (1:4, Bis-Ma/Fu group in PK30-Fu, 0.12 g Bis-Ma/1 g PK30-Fu) was added to the reaction mixture and stirred at 50 °C overnight. The amount of Bis-Ma added was based on the assumption that the actual carbonyl conversion is only 18%, instead of 20% (maximum conversion) (See appendix A1.2). Complete reagents are summarized in **Table 1**. black product mixture was dried over a Teflon tray in open air, later in a vacuum oven. The brittle sheet of thermoset product was then grinded into fine powders and dried further in the vacuum oven.

Table 1. Experimental data for sample preparation of the 5 cross-linked nanocomposite.

Code	PK30-Fu (g)	Bis-Ma (g)	CNT-CB ratio	CNT (g)	CB (g)	Carbon Fillers (g)
CNT100/CB0	7.24	0.87	100-0	0.71	0	0.71
CNT75/CB25	7.0	0.84	75-25	0.51	0.17	0.68
CNT50/CB50	7.2	0.86	50-50	0.35	0.35	0.7
CNT25/CB75	7.26	0.87	25-75	0.18	0.53	0.71
CNT0/CB100	7.24	0.87	0-100	0	0.71	0.71

2.4 Characterization of the furan-grafted polyketone and its composites

H-NMR: the furan-grafted polyketone achieved via the Paal-Knorr reaction was characterized by the Varian Mercury Plus system (400 MHz) H-NMR.

FT-IR: the 5 composites were analyzed with FT-IR Shimadzu IRTracer_100.

2.5 Sample preparation for mechanical, conductivity and shape memory testing

The powders were then molded to two different shapes, 8 mm discs and U-shape samples. A hot press was used to mold the samples at 120 °C and 80 kN for 30 mins.

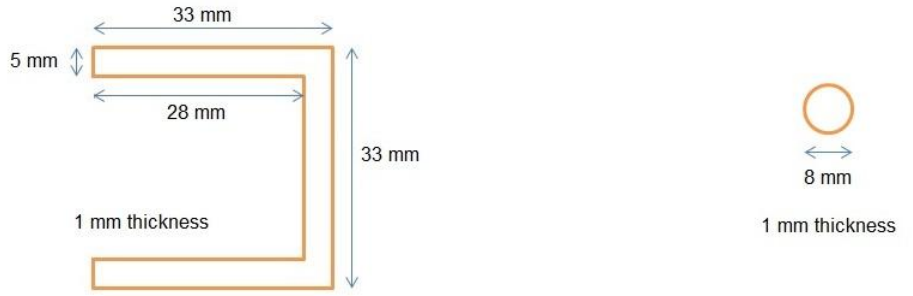

a) **b)**

Figure 6. Dimensions of the U-shape sample (a) and disc sample (b)

2.6 Conductivity and shape memory test

The U-shaped samples were used for both conductivity and shape memory tests according to the set up in **Figure 7.**

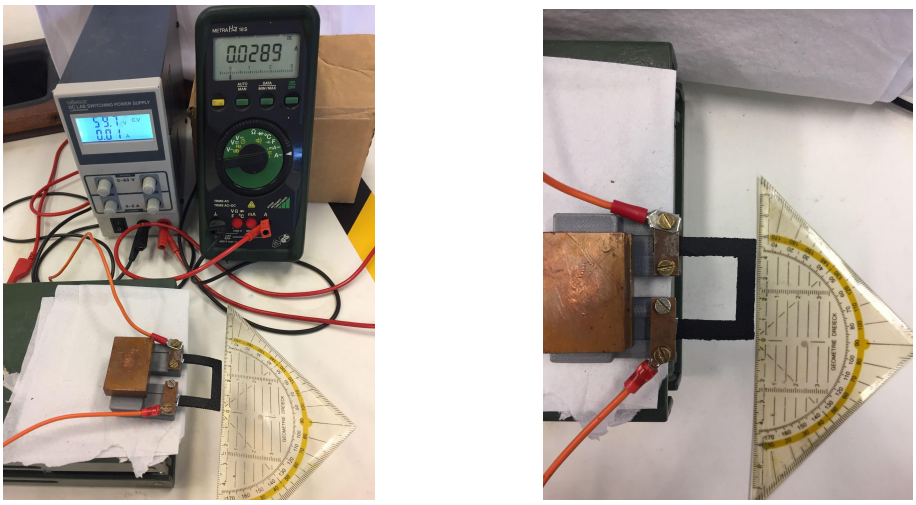

a) **b)**

Figure 7. Conductivity and shape memory test set-up: overall set-up with power source on the left and multimeter on the right side (a) and top view of the sample (b)

Voltages of 60 V were applied to the samples for 5 mins, during which the surface temperature and electrical current were measured with a visual IR thermometer and a multimeter, respectively.

Electrical conductivity (σ) was calculated according to the following *Eq.1* featuring current (I), voltage (V), length of sample (l) and cross-sectional area of sample (A).

Electrical conductivity $\sigma = \frac{I}{V} \times \frac{l}{A}$ (*Eq. 1*)

where σ = electrical resistivity [S/m], I = electrical current [A], V= voltage [V], l = length of sample [m], A= cross-sectional area of sample [m^2].

The shape memory effects induced with electricity were also measured according to the set up in **Figure 7.** Once the electrical current ran through the composite within the 5 min time-frame to approximately 100 °C (step 1), the samples were deformed at 90° to its temporary shape (step 2). While fixed at 90°, the sample was allowed to cool down to room temperature, this is done through switching off the electrical circuit. After that, the fixation was removed and 60 V voltage was applied again to trigger the shape memory effect. The sample then returns to its original shape (step 3). The overall process is shown in **Figure 8.**

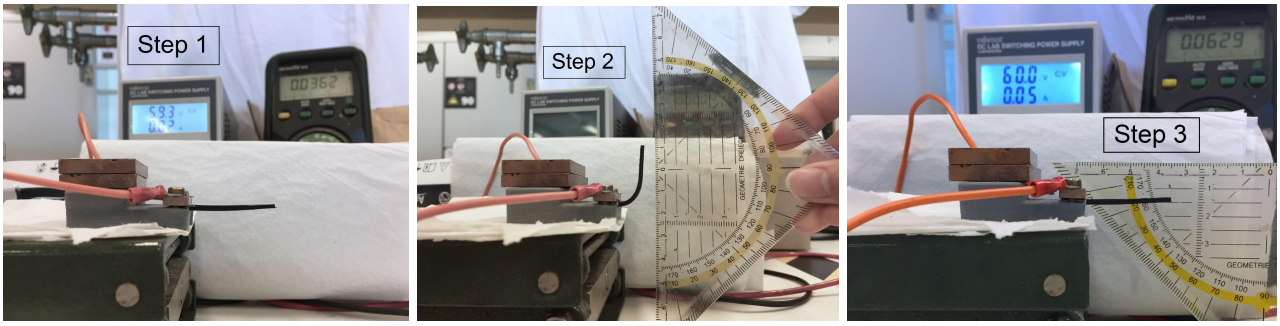

Figure 8. Shape memory test procedure: original shape (step 1), temporary shape (step 2) and recovered shape (step 3)

Shape recover rate and shape recovery ratio can be calculated for each of the samples as following:

Shape recovery ratio = $\frac{\sigma fixed - \sigma recov}{\sigma fixed}$ x 100% [%] (*Eq. 2*)

where σ_{fixed} = the fixed angle of the deformed sample [rad] and σ_{recov} = the recovered angle of the sample after stress removed [rad]

Shape recovery rate = $\frac{\sigma fixed - \sigma recov}{recov\ time}$ [rad/s] (*Eq. 3*)

where σ = the angle of the sample [rad]

2.7 Reprogramming new permanent shape and activating its shape memory effect

New permanent shape was reprogrammed through resistive heating. This was done only on one sample of CB100 formulation by heating up the sample to approximately 120 °C (50 V, 60 mA) and maintaining the heat/electric current for 3 h while the shape was held in a 90° position. After that, the stress was removed and the sample was left to stand by itself in which the angle changed down to 57°(new permanent shape). Later, the sample was deformed to horizontal shape, and the electricity was switched off, thus “freezing” the sample in its temporary state. To trigger the shape memory effect, the electrical circuit was switched on and through resistive heating, the sample recovered to its original shape (53°). The overall process is shown in **Figure 9.**

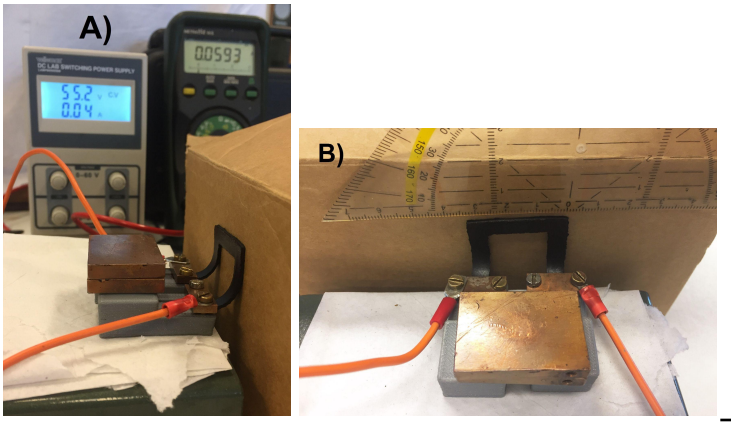

Figure 9. Programming new permanent shape set-up, the sample position was maintained at approx. 120 °C (50 V, 60 mA) for 3 h: side view (A) and top view (B)

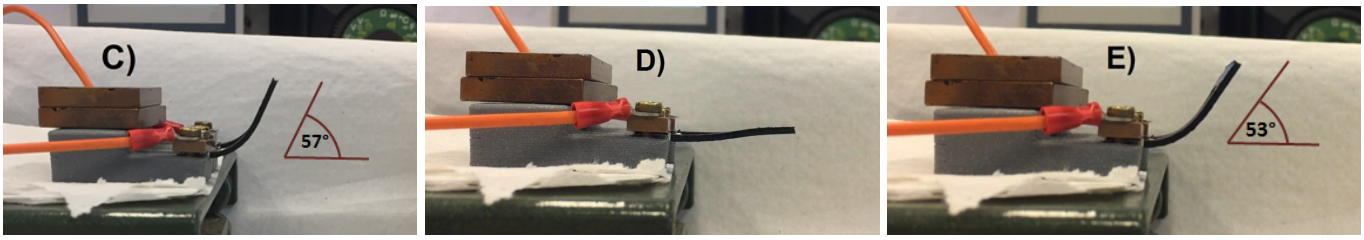

Figure 10. Shape memory effect progress of the new permanent shape: new original shape (C), temporary shape (D) and recovered shape after shape memory effect was electro-induced (E)

2.8 Rheology test for thermo-mechanical properties

The mechanical properties of the 5 formulations were analyzed using TA instrument - Hybrid Discovery HR-2 model rheometer with 8mm diameter parallel plates geometry. The 8mm disc samples were used for this analysis. First, the amplitude sweep test was conducted at a constant axial force of 7 N and oscillation frequency of 1 Hz. This was done to find a stable value (where the viscoelastic plateau is linear and horizontal) which would be used for temperature sweep in the next step. The range of strain in the amplitude sweep was between 0.001 and 10% strain. Later, storage and loss moduli were measured in between 2 different temperature sweeps of 50 and 120 °C, and both moduli were plotted against temperature. All data was processed using TRIOS software.

3. Results and Discussion

3.1 Synthesis and the final product sample preparation

Following the Paal-Knorr reaction of polyketone (PK30) with furfurylamine, H-NMR of the grafted product was taken, and is reported in **Figure 11**. Considering the H-NMR, it was confirmed that the polyketone was successfully grafted with furfurylamine with 18% 1,4-dicarbonyl conversion (C_{CO} = 0.18) (see appendix A2.2), in which this value matches with the assumption made for determining the cross-linking and composite formulation reagents (Bis-Ma and carbon fillers amount). The Paal-Knorr reaction of PK30 and furfurylamine in bulk indeed worked as the reference from Zhang et al. The four blue downfield signals between 4.5 - 7.5 ppm belong to protons on the furan group, and the red peak at 1.96 ppm is the CH_3 in the pyrrole ring. Finally, the yellow signal at 1.07 ppm represents the CH_3 on both grafted and ungrafted units.

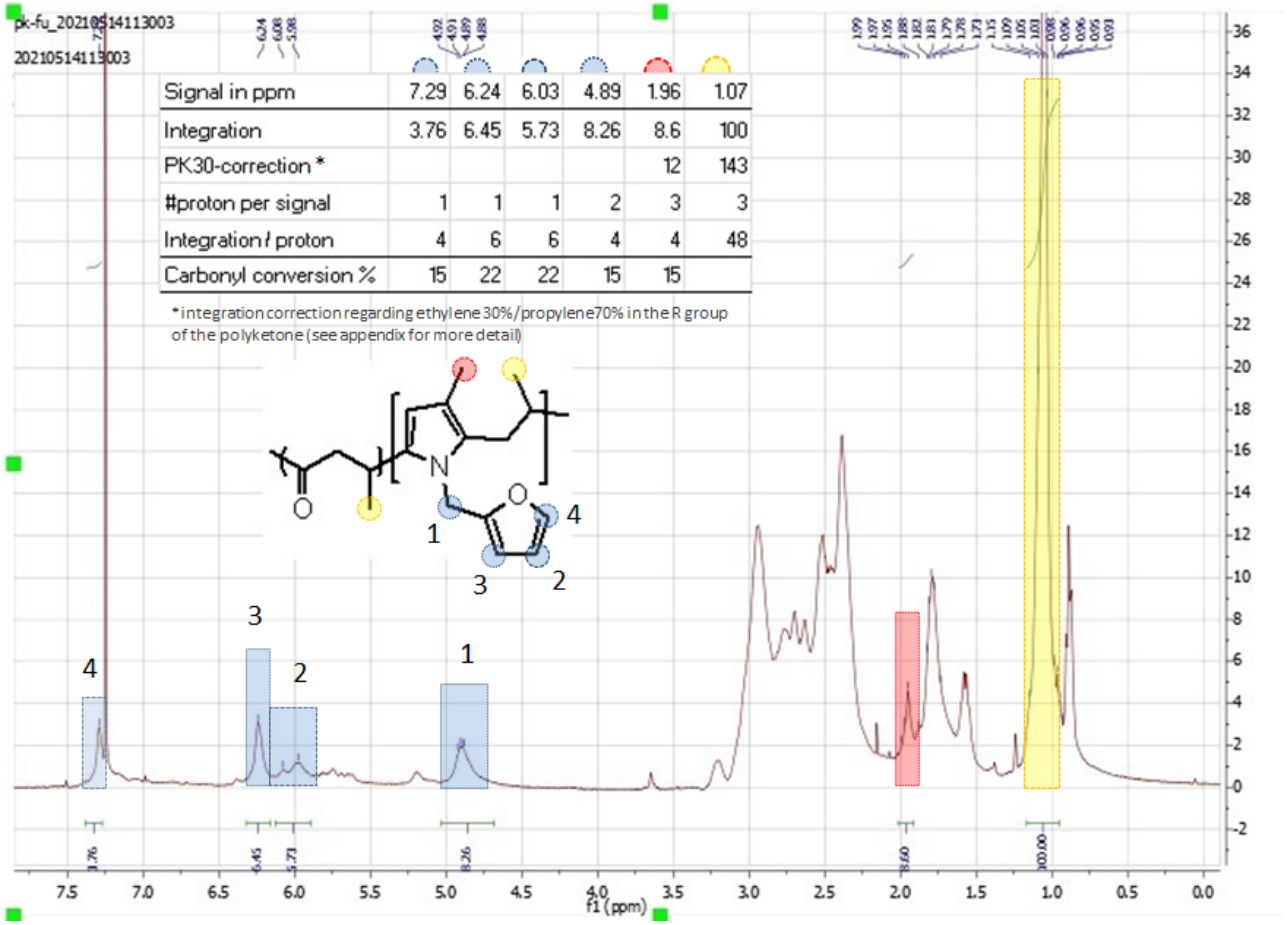

Figure 11. H-NMR of the furan-grafted polyketone: average carbonyl conversion (C_{CO}) of 18% (see appendix A2.2)

After the cross-linking and composite formulation, FT-IR was also taken for product characterization as displayed in **Figure 12**. FT-IR of the 5 composite formulations all display the ether bond formation (C-O-C) and succinimide ring of the DA adduct at 1182 cm^{-1} of the reacted furan ring through the Diels-Alder cross-linking [13,28] , and also the C-N stretching of the maleimide ring at 1378 cm^{-1} [11]. This suggests that bis-maleimide was present in the polymer system, and the Diels-Alder cross-linking reaction of furan-grafted polyketone was successful.

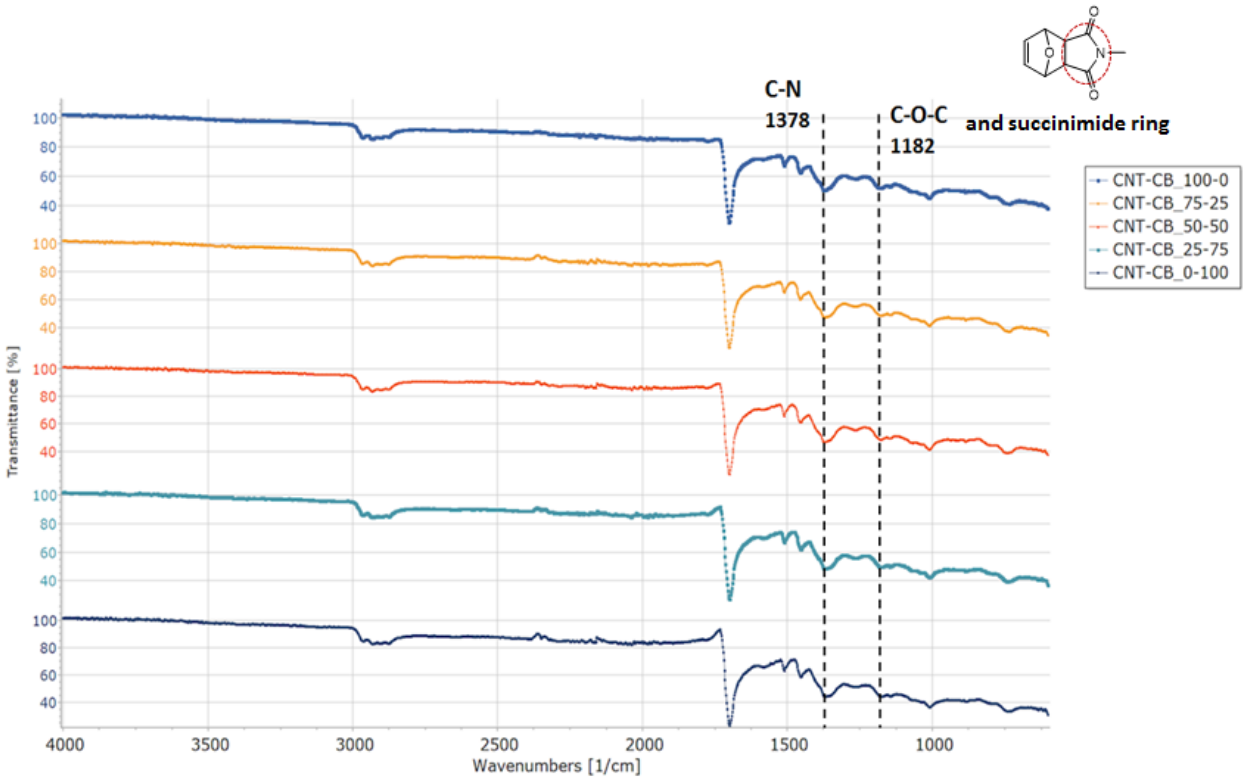

Figure 12. FT-IR of the 5 conductive composite formulations of furan-grafted polyketone (PK30-Fu) cross-linked with bis-maleimide (Bis-Ma), from top to bottom: CNT100 (100-0, navy), CNT75/CB25 (75-25, yellow), CNT50/CB50 (50-50, orange), CNT25/CB75 (25-75, turquoise) and CB100 (0-100, purple). Two important signals displayed: C-O-C ether and succinimide ring at 1182 cm^{-1} [13,28] and C-N stretch of maleimide ring at 1378 cm^{-1} [11].

3.2 Mechanical properties

Considering potential applications of the end product as robot actuators, it is therefore important that this material meets thermal and mechanical specifications. Rheology test was performed accordingly to evaluate thermo-mechanical properties of all 5 cross-linked PK30-Fu conductive composites. With thermal cycles between 120 and 50°C (retro-DA and DA temperatures), both cooling and heating were done twice. Additionally, two disc samples of the same formulation were tested, and the higher modulus of the two for each sample was taken as the representative in **Figure 13.** The complex modulus (G*), an overall resistance to deformation, also called the rigidity of the material [29], increases towards cooling, and decreases towards heating for all samples of all reps. As expected, the composite becomes less rigid and more mobile at elevated temperatures, and the graph occurs to be power law. This is due to the polymer system having less mobility and also the Diels-Alder equilibrium shifting towards a more cross-linked matrix (DA adduct) at lower temperature [14]. The overall modulus is slightly higher for both heating and cooling in the first thermal cycle compared to the latter cycle. This is because the sample was constantly pressed by the rheometer during the first cycle, resulting in the rise of the composite modulus. Although difficult to see, there is a trend for higher modulus towards more carbon black filler samples. For all cycles, the lowest complex modulus profile is CNT100/CB0 and highest complex modulus profile is the CNT0/CB100. The highest complex modulus discrepancy among the composites (outliers excluded) is approximately 5 MPa. With a great deal of overlap between the curves, it can be

concluded that the thermo-mechanical properties of different CNT/CB ratio nanocomposite is bordering on the similar values, with a slight trend towards higher modulus for CB composite.

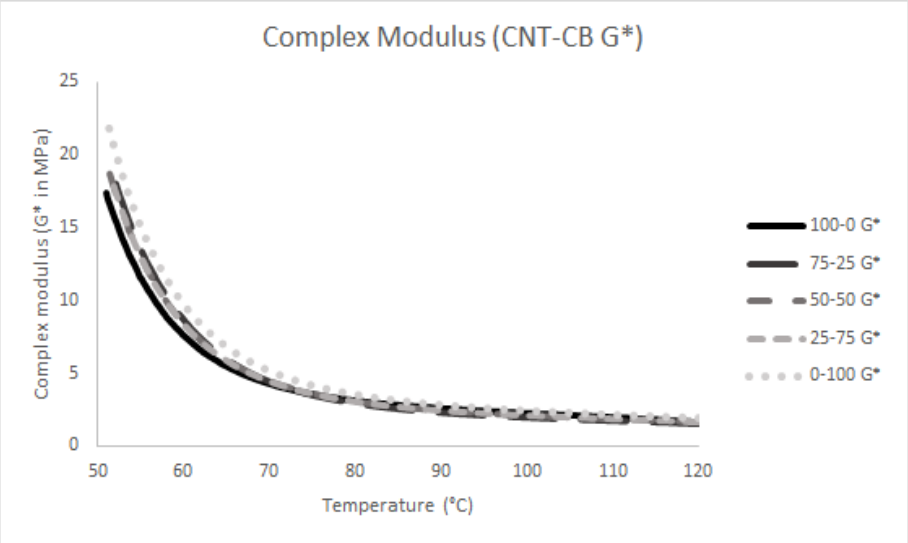

Figure 13. Thermo-mechanical profile (complex modulus (G*) representation) of the 5 composites of furan-grafted polyketone (CNT-CB) between 120-50 °C

3.3 Electrical properties

The samples were tested for conductivity according to **Figure 7**. With 60 V power for 5 mins, the resistive heating temperature profile in **Figure 14** appears to be logarithmic, as the highest temperature rise was within the first minute. Different formulations reached different maximum temperatures in a period of 5 minutes. The highest final temperature achieved (127 ± 3°C) was from CNT0/CB100 (0-100) while the lowest final temperature (82 ± 3°C) was reached with CNT100/CB0 (100-0). With approximately 45 °C difference between the two extremes, it is then up to the final product thermal and functional specifications for which CNT-CB formulation is the most suitable. There is an apparent tendency towards a higher temperature profile with increase in carbon black. However, the CNT50/CB50 (50-50) curve is unexpectedly below the CNT75/CB25 (75-25) curve. This could be due to error in dispersion of the carbon fillers in one or both of the samples where the fillers might have agglomerated together in such a way that the heating process was disrupted.

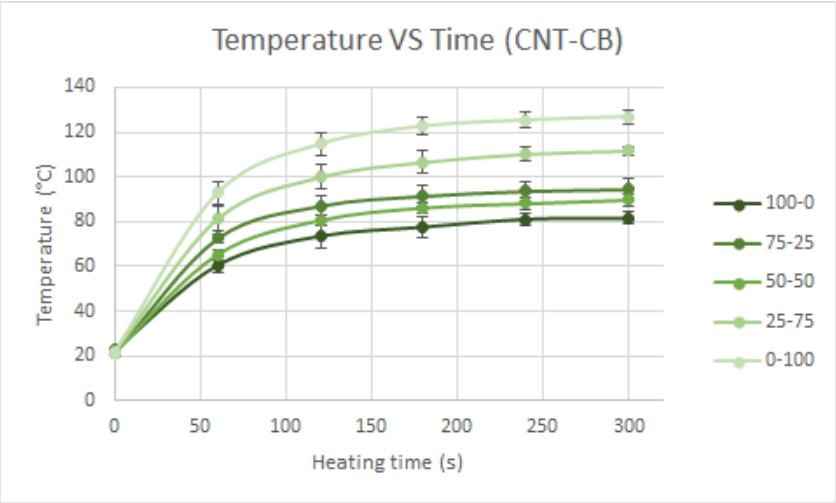

Figure 14. Temperature profile of the U-shape sample after electro-induced heating for 5 mins: CNT-CB (0-100, 75-25, 50-50, 25-75, 0-100).

There is noticeably an increasing trend in temperature, current and conductivity with more carbon black present in the sample as presented in **Figure 15.** This is as expected from the heating temperature profile previously in **Figure 14.** Since the heating is electro-induced, it is logical that the more current gets passed through the sample, the higher the temperature. In other words, the more conductive the composite sample is, the higher the temperature reached, and also the faster the heating as well (see **Figure 14.** for temperature profile). Overall, CNT0/CB100 (0-100) has the highest conductivity and also heats up the fastest among all the samples.

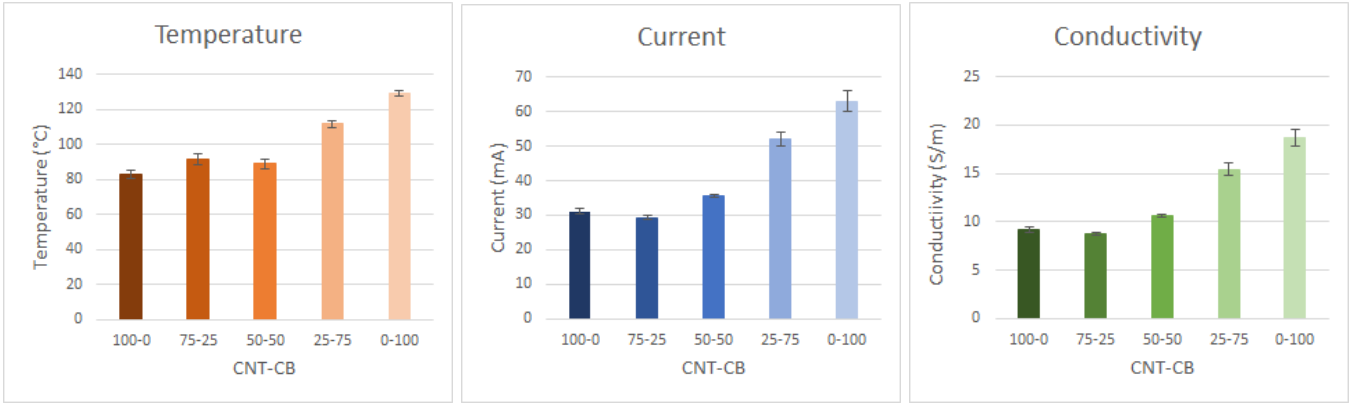

a) **b)** **c)**

Figure 15. Bar graphs of final temperature (a), electrical current (b) and conductivity (c) of the U-shape sample after electro-induced heating for 5 mins: CNT-CB (0-100, 75-25, 50-50, 25-75, 0-100).

Considering pure fillers, CNT conductivity is approximately 10^6-10^7 S/m, comparable to copper (6 x10^7 S/m) [30] whereas CB conductivity is roughly 3 x10^2 [31]. CNT is clearly more conductive than CB by several orders of magnitude. However, the result obtained in this study is the opposite, CNT is less conductive than CB. It appears that once the fillers are in the composite itself, conductivity indicated for the pure individual filler may not apply. This is most likely due to the dispersion of nanofillers within the

polymer matrix in which one or both fillers agglomerate resulting in a poorly formed conductive path with many “dead ends” contributing to overall lowered conductivity. In previous works, comparisons between the two carbon fillers and their synergistic effect were investigated in natural rubber (NR) [21], polybutylene terephthalate (PBT) of 6 wt% (66:33 CNT:CB) at 12 V [18], bis-phenol epoxy resin of 2 wt% (25:75 CNT:CB) at -10 V to 10 V [23], epoxy-based of 0.4 wt% (50:50 CNT:CB) [24]. These researches found synergies between the two co-fillers in which the percolation threshold of their system was lowered, resulting in lower resistivity and higher conductivity. Their findings and ours are incomparable as the systems are too diverse. Several parameters such as the polymer matrix, filler particle types and content, formulation process and testing conditions all contribute to the synergies between the co-fillers [23]. Although synergistic effect was not observed, it might still be attainable with different filler loading, voltage supply, or preparation process [23].

The final temperature after electro-induced heating for 5 minutes was plotted against the final current measured and also the conductivity shown in **Figure 16**. It is clear that the temperature is linearly proportional to current (also conductivity), and the graph forms a positive slope. Moreover, the formulations align in order from the least conductive CNT100/CB0 (100-0) to the most conductive CNT100/CB100 (0-100). As expected, there is a linear correlation between current and temperature within the explored range.

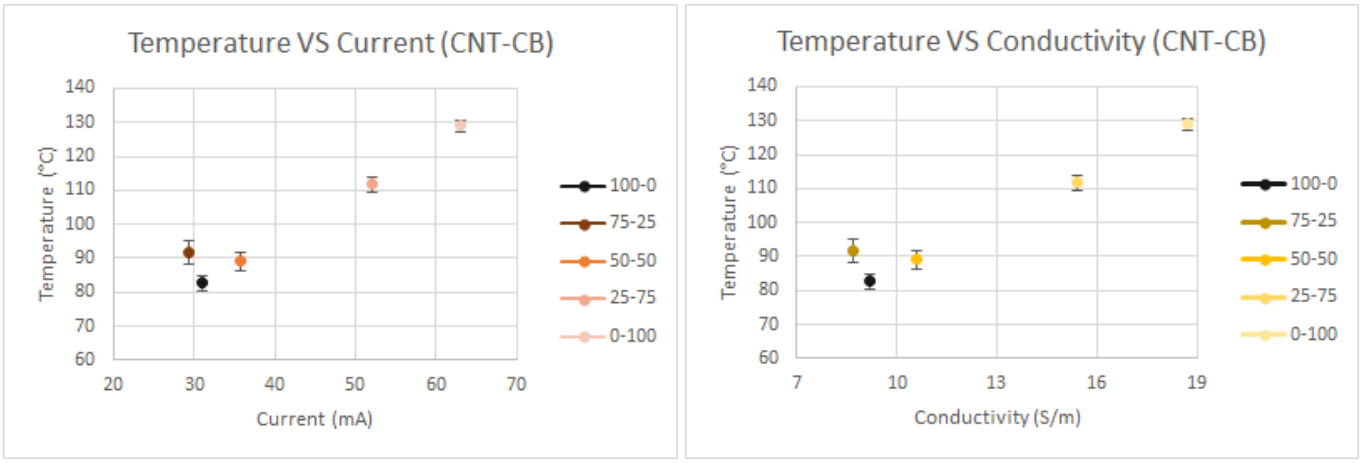

a) **b)**

Figure 16. Plot of final temperature against electrical current (a) and final temperature against conductivity (b) of the U-shape sample after electro-induced heating for 5 mins: CNT-CB (0-100, 75-25, 50-50, 25-75, 0-100).

3.4 Shape memory

First of all, it is clear that all formulations managed to recover back fully to their original horizontal shape when deformed at 90° as reported in **Figure 17 a**. The shape recovery rate in **Figure 17 b** appears to be proportional to all the previous plots including temperature, current and conductivity. The formulation with the fastest recovery rate was the CNT0/CB100 (0-100), this most likely due to the high conductivity that this sample has. Since the better the conductivity, the quicker the sample heated up, the faster the shape memory effect took place. There is also an increasing trend moving towards more carbon black, with one outlier being the CNT50/CB50 (50-50). This particular sample was the slowest to recover to the original shape. These results add a new layer towards what was already observed in other

studies [1,4,6-7,11-13] regarding shape memory polymers in which it is now possible to achieve the effect with CB or CNT/CB hybrid for the Bis-Ma cross-linked PK30-Fu system while previously done using CNT.

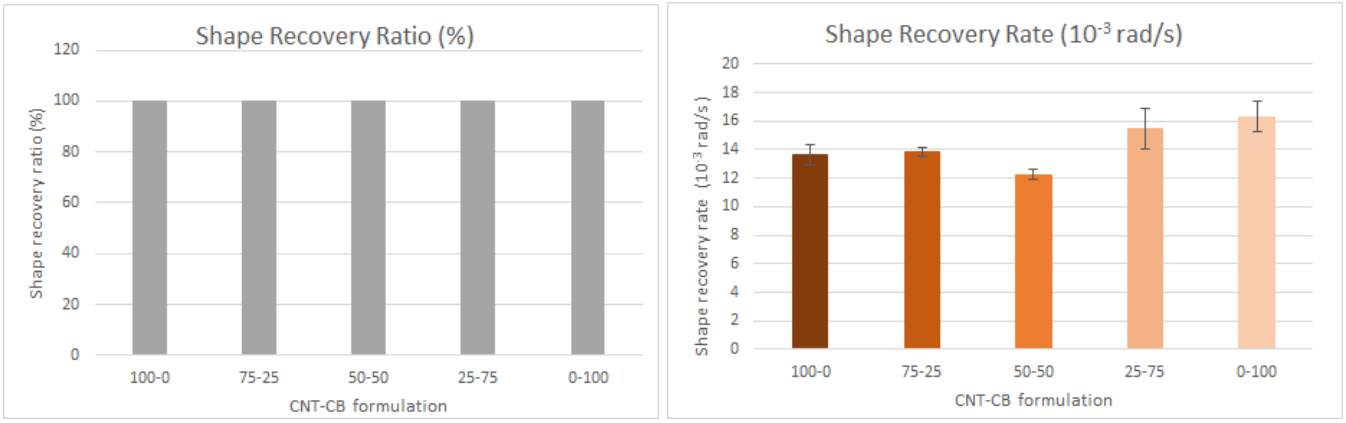

a) **b)**

Figure 17. Bar graphs of shape recovery ratio (a) and shape recovery rate (b) of the deformed (90°) U-shape sample towards original shape (horizontal, 0°): CNT-CB (0-100, 75-25, 50-50, 25-75, 0-100).

The obtained shape recovery rate was also plotted against the final temperature and also against final current (both after 5 mins heating) as displayed in **Figure 18 a, b** respectively. Both graphs exhibit correlation between recovery rate and electro-induced heating parameters. Overall, both final temperature and final current are growing with respect to the shape recovery rate, thereby confirming the verdict stated in the previous paragraph in which the greater the sample's conductivity, the faster the heating, and consequently the shape recovery rate is high.

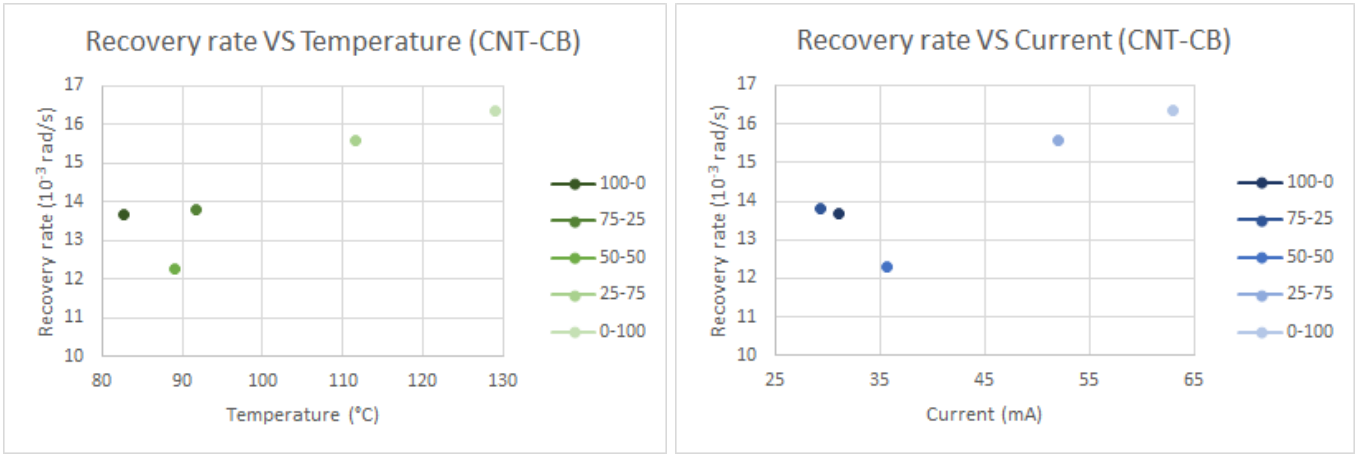

a) **b)**

Figure 18. Plot of shape recovery rate against final temperature (a) and shape recovery rate against final current (b) of the U-shape sample: CNT-CB (0-100, 75-25, 50-50, 25-75, 0-100).

3.5 Reprogrammability and its shape recovery

Since the reprogramming was only done on the most conductive sample: 100% carbon black CB100, there is no comparison between the 5 carbon composites. The reprogrammability and its shape

recoverability of the new permanent shape was also not 100%. Ideally, the new shape should be at a 90° position, but in reality, the sample was able to only stay at 57° which converts to 63% reprogrammable. Although not perfect, after deformation to a temporary shape (horizontal, 0°), the sample managed to almost recover back to its original position (53°) which counts as 93% shape recovery. This signifies that the Diels-Alder cross-linked PK-Fu network possesses network adaptability, in which the cross-linked network is able to rearrange itself to a stable new structure. This is an extremely valuable characteristic as a thermoset. Moreover, the effect was electro-induced and not through conventional heating, making this material highly versatile to many applications. Failures in the reprogramming might be due to the dispersion of the carbon filler, as some area in the cross-linked network might be obstructed by the filler in such a way that the network is not fully mobile enough to adapt to the new position effectively, resulting in partially reprogrammed shape. Or it could simply be that either reprogramming time or temperature had to be adjusted to effectively promote the reassociation of the cross-linkages through both retro-Diels-Alder and Diels-Alder reaction.

3.6 Economics

As previously discussed, the cost of carbon nanotubes is far greater than the cost of carbon black. Multiwall-carbon nanotubes are approximately 2900 €/kg [25] whereas conductive carbon black is about 120 €/kg [26]. Crude analysis of raw materials price for the conductive composites is displayed in **Figure 19**. The graph depicts prices (€/kg) of the co-fillers (CNT/CB) in 3 different categories: general polyketone composite price [32], most common polymer composites including polypropylene (PP), polyethylene - high density (HDPE), polyamide 12 (PA12) and polystyrene (PS) [33], and lastly only conductive CNT/CB fillers price [25-26]. The polymers depicted here are raw and uncross-linked, therefore the prices in all 3 categories are almost identical as the raw polymer price is insignificant compared to the nanofillers. As predicted, CNT-filled nanocomposite is considerably more expensive than the CB-filled as the pure CNT cost is 230 € per kg composite while CB price is only 10 € per kg composite, and the other formulations fall linearly in between. The raw material cost is drastically dropping towards more CB, highlighting the significance of this study regarding the economics of the electro-active carbon composite.

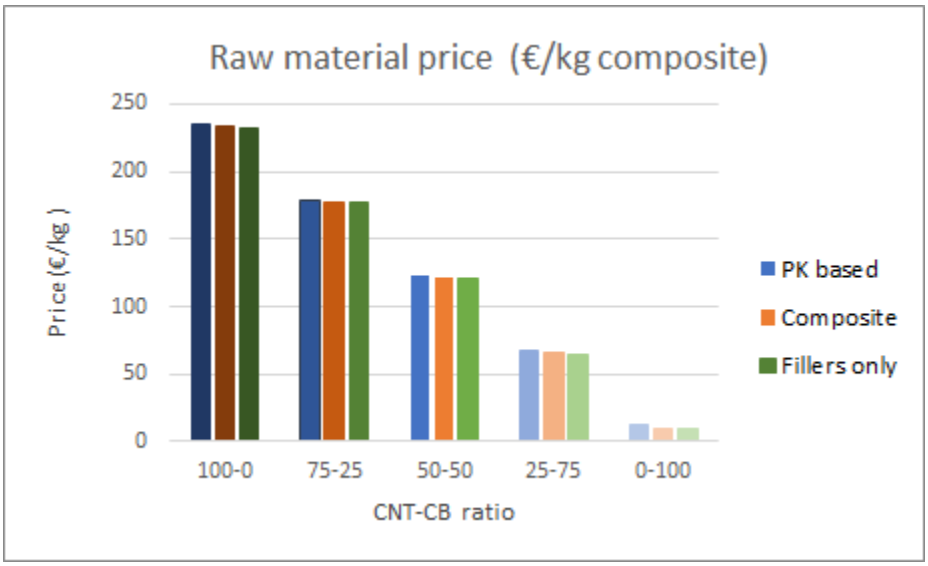

Figure 19. Bar graphs of raw materials price (€/kg composite product) on the basis of polyketone composite (blue), most popular polymers composite (PP, HDPE, PA12 and PS) (orange) and fillers only (green) [25-26,32-33]: CNT-CB (0-100, 75-25, 50-50, 25-75, 0-100).

In this project, carbon black filled nanocomposite achieved higher degree of conductivity and shape memory recovery rate. The formulations align in order from the lowest, CNT100/CB0 (100-0) to the highest, CNT0/CB100 (0-100) for conductivity and shape recovery rate. In **Figure 14**, the energy put in the system is the same (60 V) for all samples, yet the highest temperature reached was from the CNT0/CB100. Thus, less voltage is needed to heat up the CNT0/CB100 to the same temperature reached by CNT100/CB0, making the CNT0/CB100 more energy efficient and costing less during the end product operation. Considering all these, not only that carbon black is more economical, its relevant performance investigated in this study is superior to that of the carbon nanotube.

4. Future prospects

The results obtained including mechanical and electrical properties, shape memory effect, shape reprogrammability and the economics only applies to the specific system (Bis-Ma cross-linked PK30-Fu with 8 wt% CNT/CB) explored in this study. As mentioned above, different results were gathered by previous investigations on CNT/CB filled polymer composite [18,21,23,24]. The observed characteristics are not universal, and whether the findings will be applicable to other systems as well is up to how similar it is compared to our system. Therefore, the performance, along with the economic aspect still needs further exploration should diverse results appear for new experimental conditions. Moreover, the conductive fillers (CNT/CB) in the final composite samples were tested only on macroscopic level. The nanofillers behaviors and interactions within the polymeric system should also be studied microscopically to provide further explanation and clarification for the macroscopic results. This can be done through microscopy to see the dispersions of the two fillers (CNT and CB) in nano-scale. Unfortunately due to time constraints, self-healing tests on this conductive nanocomposite were not performed. For further completion on this research topic, this area of smart properties still needs to be explored.

5. Conclusion

For the Diels-Alder based CNT/CB electroactive nanocomposite, there is a linear positive correlation between surface temperature detected, current and conductivity. Samples with more CB content exhibit greater current and conductivity, and higher temperature profile as a result of successful resistive heating. All composite samples possess similar complex modulus (G*) and a high degree of shape memory ability with 100% recovery ratio. The highest recovery rate was obtained from the pure CB sample in which the temperature and current also show linear interrelationship. Partial reprogrammability and full shape recovery for the new permanent shape was achieved with the most conductive sample (CNT0/CB100 or 0-100). No synergies were found between CNT and CB as co-fillers for the system explored. Lastly, no compromisation needed to be considered regarding cost/properties relationship as the most conductive with highest shape recovery rate (CNT0/CB100 or 0-100) is also the most economical composite formulation. These findings contribute to existing literature such that many features were further investigated for this specific electroactive thermoset with the incorporation of a more economical conductive filler, carbon black.

Acknowledgments

I would like to express my sincere thanks, gratitude and appreciation towards the following people who majorly contributed towards the completion of this bachelor thesis project:

Dr. Ranjita Bose, my main supervisor and the bachelor research course coordinator, who is always providing us with resources and eager to help with any questions or troubles.

Felipe Orozco Gutierrez, my primary supervisor for his patience, guidance and encouragement. My research would not have been possible without the insights and support he has provided me throughout this project.

Laboratory staff members who organized the laboratories such that it was possible for us to safely carry out the experiments, even during the corona pandemic.

Laboratory assistants and technical staff members for characterizations needed for the research.

Researchers in Bose group for sharing their knowledge and experience for further improvements of my work.

Fellow friends and colleagues who have always been helping and aiding me throughout the entire journey of my bachelor study.

Last but not least, I would like to thank my family who never fails to believe in me.

References

[1] Lewis, C. L., & Dell, E. M. (2016). A review of shape memory polymers bearing reversible binding groups. *Journal of Polymer Science Part B: Polymer Physics*, *54*(14), 1340–1364. https://doi.org/10.1002/polb.23994

[2] Delaey, J., Dubruel, P., & Van Vlierberghe, S. (2020). Shape-memory polymers for biomedical applications. *Advanced Functional Materials*, *30*(44).

[3] Lendlein, A., & Langer, R. (2002). Biodegradable, elastic shape-memory polymers for potential biomedical applications. *Science (New York, N.y.)*, *296*(5573), 1673–6.

[4] Scalet, G. (2020). Two-way and multiple-way shape memory polymers for soft robotics: an overview. *Actuators*, *9*(1), 10–10. https://doi.org/10.3390/act9010010

[5] Menon, A. V., Madras, G., & Bose, S. (2019). The journey of self-healing and shape memory polyurethanes from bench to translational research. *Polymer Chemistry*, *10*(32), 4370–4388. https://doi.org/10.1039/c9py00854c

[6] Lima, G. M. R., Orozco, F., Picchioni, F., Moreno-Villoslada, I., Pucci, A., Bose, R. K., & Araya-Hermosilla, R. (2019). Electrically Self-Healing Thermoset MWCNTs Composites Based on Diels-Alder and Hydrogen Bonds. *Polymers*, *11*(11), [1885]. https://doi.org/10.3390/polym11111885

[7] Oliver, K., Seddon, A., & Trask, R. S. (2016). Morphing in nature and beyond: a review of natural and synthetic shape-changing materials and mechanisms. *Journal of Materials Science : Full Set - Includes `Journal of Materials Science Letters'*, *51*(24), 10663–10689. https://doi.org/10.1007/s10853-016-0295-8

[8] Vollhardt, K., & Schore, N. (2007). *Organic chemistry: structure and function*. New York, N.Y: Freeman.

[9] Mark, H., & Seidel, A. (2014). *Encyclopedia of polymer science and technology*. Hoboken, NJ: Wiley.

[10] White, S. R., Sottos, N. R., Geubelle, P. H., Moore, J. S., Kessler, M. R., Sriram, S. R., … Viswanathan, S. (2001). Autonomic healing of polymer composites. *Nature : International Weekly Journal of Science*, *409*(6822), 794–797. https://doi.org/10.1038/35057232

[11] Toncelli, C. (2013). Functional polymers from alternating aliphatic polyketones: synthesis and applications. s.n.

[12] Araya-Hermosilla, R., Pucci, A., Raffa, P., Santosa, D., Pescarmona, P. P., Gengler, R. Y. N., … Picchioni, F. (2018). Electrically-responsive reversible polyketone/mwcnt network through diels-alder chemistry. *Polymers*, *10*(10). https://doi.org/10.3390/polym10101076
[13] Zhang, Y., Broekhuis, A. A., & Picchioni, F. (2009). Thermally self-healing polymeric materials: the next step to recycling thermoset polymers? *Macromolecules*, *42*(6), 1906–1912.
[14] Polgar, L. M., van Duin, M., Broekhuis, A. A., & Picchioni, F. (2015). Use of diels-alder chemistry for thermoreversible cross-linking of rubbers: the next step toward recycling of rubber products? *Macromolecules*, *48*(19), 7096–7105.
[15] Canadell, J., Fischer, H., De With, G., & van Benthem, R. A. T. M. (2010). Stereoisomeric effects in thermo-remendable polymer networks based on diels-alder crosslink reactions. *Journal of Polymer Science Part a: Polymer Chemistry*, *48*(15), 3456–3467. https://doi.org/10.1002/pola.24134
[16] Liu, Y., Lv, H., Lan, X., Leng, J., & Du, S. (2009). Review of electro-active shape-memory polymer composite. *Composites Science and Technology*, *69*(13), 2064–2068. https://doi.org/10.1016/j.compscitech.2008.08.016
[17] Nicola, M., Lorenzo, M. P., Rodrigo, A.-H., Francesco, P., Patrizio, R., & Andrea, P. (2018). Effect of the polyketone aromatic pendent groups on the electrical conductivity of the derived mwcnts-based nanocomposites. *Polymers*, *10*(6). https://doi.org/10.3390/polym10060618
[18] Dorigato, A., Brugnara, M., & Pegoretti, A. (2017). Synergistic effects of carbon black and carbon nanotubes on the electrical resistivity of poly(butylene-terephthalate) nanocomposites. *Advances In Polymer Technology*, *37*(6), 1744-1754. doi: 10.1002/adv.21833.
[19] Sumfleth, J., Adroher, X., & Schulte, K. (2009). Synergistic effects in network formation and electrical properties of hybrid epoxy nanocomposites containing multi-wall carbon nanotubes and carbon black. *Journal Of Materials Science*, *44*(12), 3241-3247. doi: 10.1007/s10853-009-3434-7
[20] Ma, P., Liu, M., Zhang, H., Wang, S., Wang, R., & Wang, K. et al. (2009). Enhanced Electrical Conductivity of Nanocomposites Containing Hybrid Fillers of Carbon Nanotubes and Carbon Black. *ACS Applied Materials & Interfaces*, *1*(5), 1090-1096. doi: 10.1021/am9000503
[21] Nakaramontri, Y., Pichaiyut, S., Wisunthorn, S., & Nakason, C. (2017). Hybrid carbon nanotubes and conductive carbon black in natural rubber composites to enhance electrical conductivity by reducing gaps separating carbon nanotube encapsulates. *European Polymer Journal*, *90*, 467-484. doi: 10.1016/j.eurpolymj.2017.03.029
[22] Zhang, S., Lin, L., Deng, H., Gao, X., Bilotti, E., & Peijs, T. et al. (2012). Synergistic effect in conductive networks constructed with carbon nanofillers in different dimensions. *Express Polymer Letters*, *6*(2), 159-168. doi: 10.3144/expresspolymlett.2012.17
[23] Zhang, C., Sun, L., Huang, B., Yang, X., Chu, Y., & Zhan, B. (2019). Electrical and mechanical properties of cnt/cb dual filler conductive adhesives (dfcas) for automotive multi-material joints. *Composite Structures*, *225*. https://doi.org/10.1016/j.compstruct.2019.111183
[24] Szeluga, U., Kumanek, B., & Trzebicka, B. (2015). Synergy in hybrid polymer/nanocarbon composites. a review. *Composites Part A*, *73*, 204–231. https://doi.org/10.1016/j.compositesa.2015.02.021
[25] Carbon Nanotubes - Price - Chinese Academy of Sciences, Chengdu Organic Chemistry Co., Ltd. (2021).
[26] Ketjenblack EC-600JD Electroconductive carbon black. (2021).

[27] Eatemadi, A., Daraee, H., Karimkhanloo, H., Kouhi, M., Zarghami, N., Akbarzadeh, A., … Joo, S. W. (2014). Carbon nanotubes: properties, synthesis, purification, and medical applications. *Nanoscale Research Letters*, *9*(1), 1–13. https://doi.org/10.1186/1556-276X-9-393
[28] Orozco, F., Niyazov, Z., Garnier, T., Migliore, N., Zdvizhkov, A. T., Raffa, P., Moreno-Villoslada, I., Picchioni, F., & Bose, R. K. (2021). Maleimide self-reaction in furan/maleimide-based reversibly crosslinked polyketones: processing limitation or potential advantage? *Molecules (Basel, Switzerland)*, *26*(8). https://doi.org/10.3390/molecules26082230
[29] Cunningham, N. (2021). Viscosity & Rheology Glossary from the Centre for Industrial Rheology.
[30] Wu, H.-C., Chang, X., Liu, L., Zhao, F., & Zhao, Y. (2010). Chemistry of carbon nanotubes in biomedical applications. *J. Mater. Chem*, *20*(6), 1036–1052. https://doi.org/10.1039/B911099M
[31] KETJENBLACK Highly Electro-Conductive Carbon Black | Lion Specialty Chemicals Co., Ltd. (2021).
[32] Polyketone Resin Price - Buy Cheap Polyketone Resin At Low Price On Made-in-China.com. (2021).
[33] New Media Publisher GmbH, K. (2021). Raw Materials & Prices.

Appendix

A1. Experimental Calculation:

A1.1 Paal-Knorr reaction - Furfuryl amine amount to obtain maximum carbonyl conversion of 20%

Average molar mass of the repeating unit (double carbonyl dimer), considering the ethylene30%/propylene70%:

$M_{PK} = (M_{PK,Et} \times 30\%) + (M_{PK,Pr} \times 70\%) = (112 \frac{g}{mol} \times 30\%) + (140 \frac{g}{mol} \times 70\%) = 131.6 \frac{g}{mol}$

20% carbonyl conversion, meaning out of 100 repeating dimer unit (PK dimer), 20 of those will react with equal amount of furfurylamine (FFA):

$\frac{1\ g\ PK\ dimer}{1} \times \frac{1\ mol\ PK\ dimer}{131.6\ g} \times \frac{20\ mol\ FFA}{100\ mol\ PK\ dimer} \times \frac{97.12\ g\ FFA}{1\ mol}$ = 0.15 g furfurylamine for 1 g PK dimer

For 48.51 g PK dimer: (0.15 g FFA) x (48.51 g PK dimer) = 7.16 g furfurylamine

A1.2 Crosslinking and conductive filler formulation - Assume 18% carbonyl conversion, Furan/Bis-Ma ratio of 4/1, and carbon filler of 8 wt%

Average molar mass of the furan group repeating unit, considering the ethylene30%/propylene70%:

$M_{Fu\text{-}unit} = (M_{Fu,Et} \times 30\%) + (M_{Fu,Pr} \times 70\%) = (159 \frac{g}{mol} \times 30\%) + (187 \frac{g}{mol} \times 70\%) = 178.6 \frac{g}{mol}$

Average molar mass of the furan-grafted polyketone repeating unit , assuming 18% carbonyl conversion, meaning that there will be 18% furan group unit and 82% polyketone dimer units (E/P of 30/70):

$M_{PK\text{-}Fu} = (M_{Fu\text{-}unit} \times 18\%) + (M_{PK} \times 82\%) = (187.6 \frac{g}{mol} \times 18\%) + (131.6 \frac{g}{mol} \times 82\%) = 140 \frac{g}{mol}$

Since carbonyl conversion is 18%, 18 furan units are present out of 100 repeating units, and Furan/Bis-Ma ratio of 4/1, then amount of Bis-Ma needed for a 7 gram PK-Fu sample:

$\frac{18\ mol\ Fu{-}unit}{100\ mol\ PK{-}Fu} \times \frac{1\ mol\ PK{-}Fu}{140\ g\ PK{-}Fu} \times \frac{1\ mol\ Bis{-}Ma}{4\ mol\ Fu{-}unit} \times \frac{358.3\ g\ Bis{-}Ma}{1\ mol\ Bis{-}Ma} \times 7$ g PK-Fu = 0.84 g Bis-Ma

Conductive carbon filler mass calculation for 8 wt% composite:

$$\frac{8\ wt\%}{100\% - 8\ wt\%} = \frac{Mass\ filler}{Total\ mass - Mass\ filler} = \frac{Mass\ filler}{PK{-}Fu + Bis{-}Ma};$$

Mass filler = $\frac{8\ wt\%}{100\% - 8\ wt\%}$ X (PK-Fu mass + Bis-Ma mass)

= $\frac{8\ wt\%}{100\% - 8\ wt\%}$ x (7 g + 0.84 g) = 0.68 g carbon filler

A2. H-NMR related calculations:

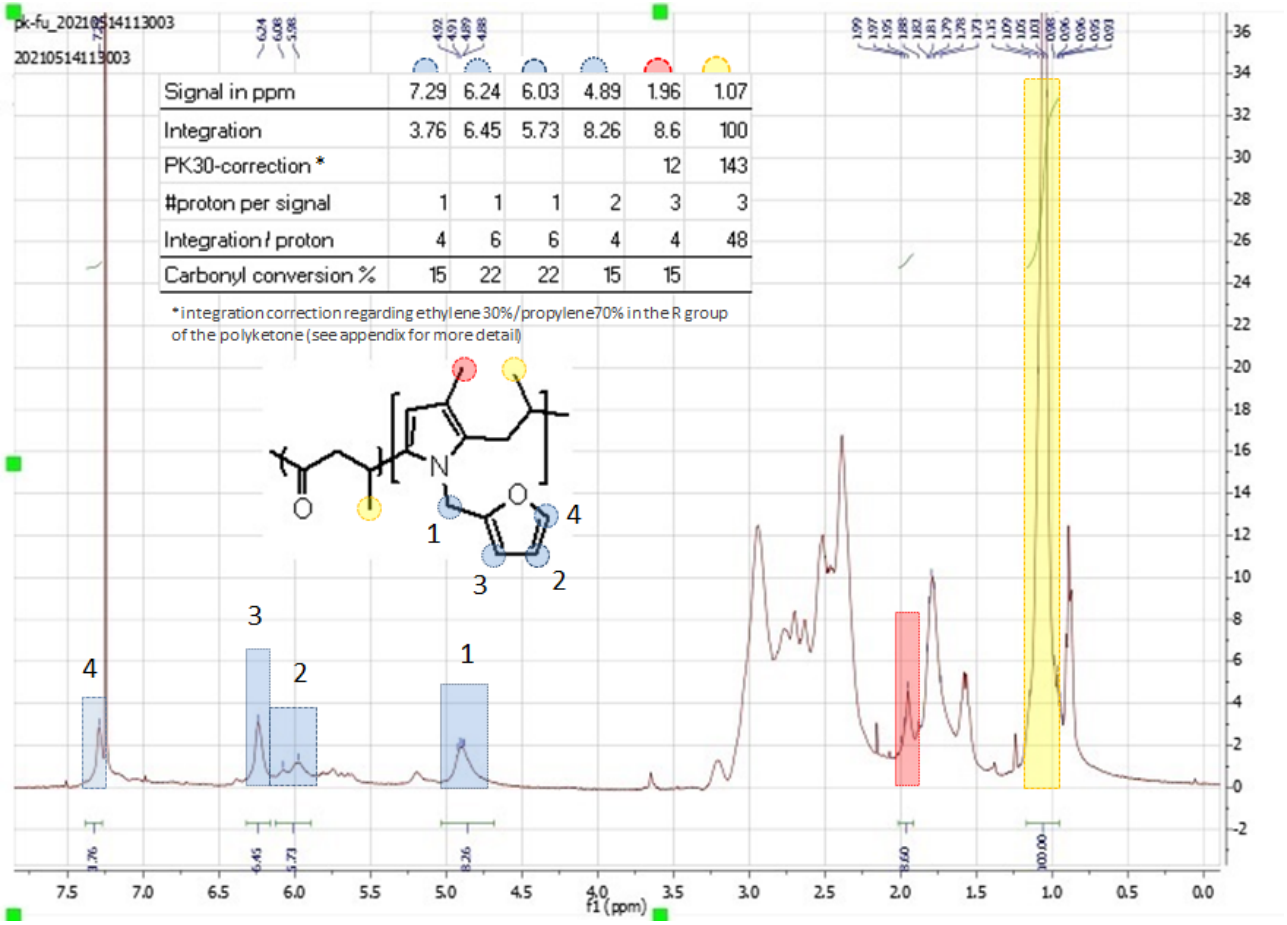

Figure A2. H-NMR spectrum of the furan-grafted polyketone: average carbonyl conversion (C_{CO}) of 18%

A2.1 PK30-correction calculation for alkyl hydrogens based on ethylene/propylene% of polyketone

PK30 correction calculation is for the yellow peak and for the red peak. The yellow signal at 1.07 ppm represents the CH_3 on both grafted and ungrafted dimer, and the red signal at 1.96 ppm represents the CH_3 on the pyrrole ring. Since both belong to the R group with ethylene30%/propylene70% ratio (instead of propylene100%), the integration had to be adjusted.

The ratio for the this relationship is $\frac{70\%}{100\%} = \frac{i\ (ungrafted\ dimer)}{i\ (PK30{-}correction)}$; therefore

i (PK30-correction) = $\frac{i\ (ungrafted\ dimer)}{1}$ x $\frac{100\%}{70\%}$

For example, the yellow signal at 1.07 ppm was adjusted according to the above formula:

$$i\ (\text{PK30-correction})_{yellow} = \frac{100}{1} \times \frac{100\%}{70\%} = 143$$

A2.2 Carbonyl conversion C_{CO} calculation from H-NMR spectrum of PK-Fu

Average carbonyl conversion (C_{CO}) can be calculated using this following formula:

$$C_{CO} = \frac{i\ (grafted)}{i\ (grafted) + \frac{i\ (ungrafted\ dimer) - i\ (grafted)}{2}} \times 100\%$$

Where i (grafted) represents the integration/proton of signals that belong to the grafted unit which refers to the red signal at 1.96 ppm and all the blue ones at 4.89, 6.03, 6.24 and 7.29 ppm ;
And i (ungrafted dimer) refers to the integration/protom of the yellow peak at 1.07 ppm.

For example, C_{CO} of for the blue signal 4 at 7.29 ppm in one the furan ring will be calculated according to the above formula:

$$C_{CO,\,4} = \frac{4}{4 + \frac{48 - 4}{2}} \times 100\% = 15\%$$

The overall carbonyl conversion (C_{CO}) is taken as the average of the 5 individual conversions of 15%, 22%, 22%, 15% and 15% which is 18% overall.

A3. Conductivity calculation:

$$\text{Electrical conductivity } \sigma = \frac{I}{V} \times \frac{l}{A} \qquad (Eq.\ 1)$$

where σ = electrical resistivity [S/m], I = electrical current [A], V= voltage [V], l = length of sample [m], A= cross-sectional area of sample [m^2].
For example, conductivity of the 100% carbon nanotube (CNT100 or 100-0 in **Figure 15c**) will be determined based on the above equation:

$$\text{Electrical conductivity } \sigma = \frac{31x10^{-3}\ A}{60\ V} \mathbf{X} \frac{(30.5+28+30.5)x10^{-3}\ m}{(1x10^{-3})\ x\ (5x10^{-3})\ m^2} = 9.2\ \text{S/m}$$

A4. Mechanical properties from rheology test:

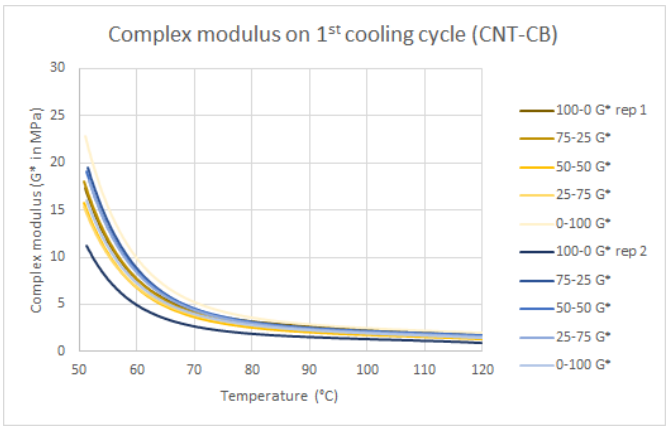

a)

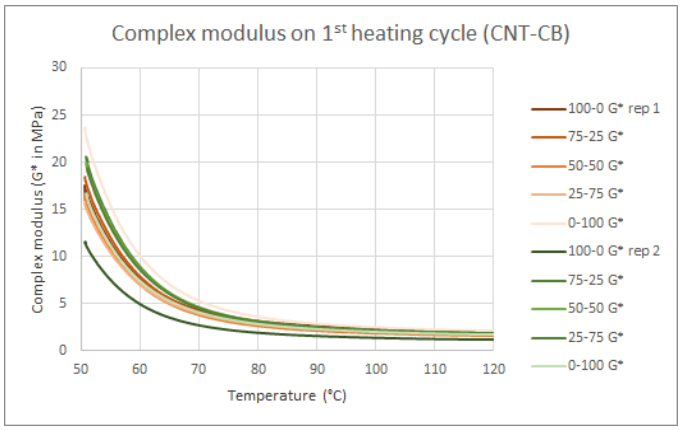

b)

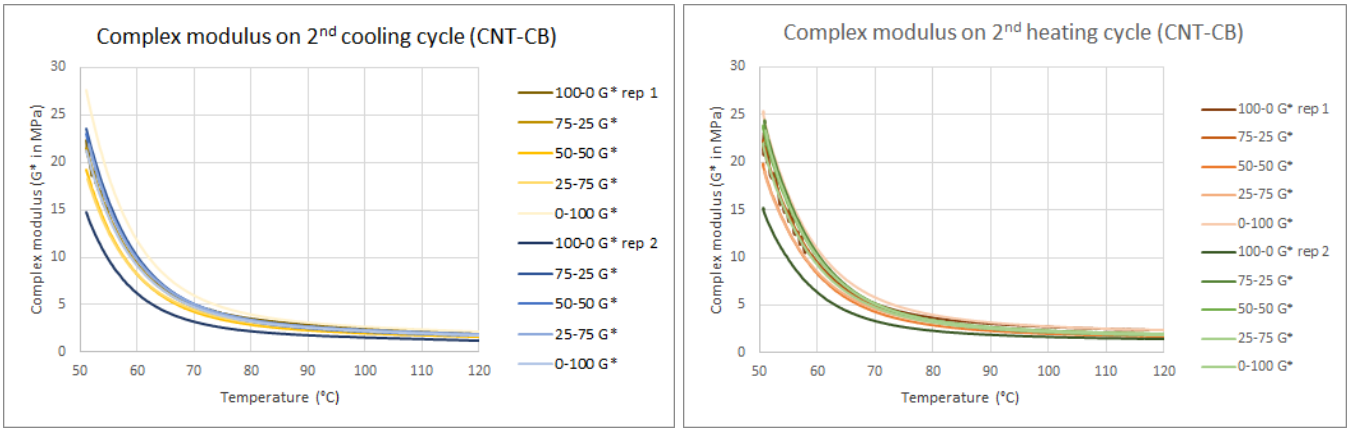

c) **d)**

Figure A4. Thermo-mechanical profile of the 5 composite formulations of furan-grafted polyketone (CNT-CB) with 2 thermal cycles ranged between 120-50 °C: first cooling cycle (a), first heating cycle (b), second cooling cycle (c) and second heating cycle (d). Two 8mm disc samples of the same formulation evaluated (rep 1 and rep 2).

With thermal cycles between 120 and 50°C (retro-DA and DA temperatures), both cooling and heating were done twice. Additionally, two disc samples of the same formulation were tested, thus rep 1 and rep 2. The overall modulus is slightly higher for both heating and cooling in the first thermal cycle in ***Figure A4 a and b*** compared to the latter cycle in ***Figure A4 c and d***. This is because the sample was constantly pressed by the rheometer during the first cycle, resulting in the rise of the composite stiffness. For all cycles, the lowest complex modulus profile is CNT100/CB0 (100-0 rep 2) and highest complex modulus profile is the CNT0/CB100 (0-100 rep1). The highest complex modulus discrepancy among the composites (outliers excluded) is approximately 5 MPa.